

“Conductive” yttria-stabilized zirconia as an epitaxial template for oxide heterostructures

C. Caspers, A. Gloskovskii, W. Drube, C. M. Schneider, and M. Müller

Citation: *Journal of Applied Physics* **115**, 17C111 (2014); doi: 10.1063/1.4863803

View online: <http://dx.doi.org/10.1063/1.4863803>

View Table of Contents: <http://scitation.aip.org/content/aip/journal/jap/115/17?ver=pdfcov>

Published by the AIP Publishing

Articles you may be interested in

[Improved ionic conductivity in strained yttria-stabilized zirconia thin films](#)

Appl. Phys. Lett. **102**, 143901 (2013); 10.1063/1.4801649

[Swift heavy ion-induced swelling and damage in yttria-stabilized zirconia](#)

J. Appl. Phys. **101**, 073501 (2007); 10.1063/1.2714651

[Large low-field magnetoresistance observed in twinned La \$2/3\$ Ca \$1/3\$ MnO \$3\$ thin films epitaxially grown on yttria-stabilized zirconia-buffered silicon on insulator substrates](#)

Appl. Phys. Lett. **86**, 112514 (2005); 10.1063/1.1875766

[Dislocation-enhanced ionic conductivity of yttria-stabilized zirconia](#)

Appl. Phys. Lett. **82**, 877 (2003); 10.1063/1.1544440

[Electrical conductivity relaxation in thin-film yttria-stabilized zirconia](#)

Appl. Phys. Lett. **78**, 610 (2001); 10.1063/1.1343852

The advertisement features a dark blue background with a film strip graphic on the left side. The text is centered and reads: 'Not all AFMs are created equal' in orange, 'Asylum Research Cypher™ AFMs' in white, and 'There's no other AFM like Cypher' in orange. Below the text is the website 'www.AsylumResearch.com/NoOtherAFMLikeIt' and the Oxford Instruments logo with the tagline 'The Business of Science®'.

“Conductive” yttria-stabilized zirconia as an epitaxial template for oxide heterostructures

C. Caspers,¹ A. Gloskovskii,² W. Drube,² C. M. Schneider,^{1,3} and M. Müller^{1,a)}

¹Peter Grünberg Institut (PGI-6), Forschungszentrum Jülich, 52425 Jülich, Germany

²DESY Photon Science, Deutsches Elektronen-Synchrotron, 22603 Hamburg, Germany

³Fakultät für Physik and Center for Nanointegration Duisburg-Essen (CeNIDE), 47048 Duisburg, Germany

(Presented 8 November 2013; received 23 September 2013; accepted 1 November 2013; published online 31 January 2014)

We report an *in situ* thermochemical treatment that significantly increases the macroscopic electrical conductivity of insulating yttria-stabilized zirconia (YSZ) (001) single-crystalline substrates. We demonstrate the high-quality surface crystalline structure of the resulting “conductive” cYSZ (001) by low- and high-energy electron diffraction. Soft- and hard X-ray photoemission spectroscopy measurements reveal a sizable reduction of Zr cations to a metallic state and their homogeneous distribution within the cYSZ. We discuss the correlation between the microscopic chemical processes leading to the increased macroscopic metallicity. Finally, the heteroepitaxial growth of a functional magnetic oxide model system, ultrathin EuO on cYSZ (001), was demonstrated. cYSZ (001) thereby enables both high quality oxide heteroepitaxy and the advanced sample characterization by high electron-fluence characterization techniques. © 2014 AIP Publishing LLC. [<http://dx.doi.org/10.1063/1.4863803>]

The cubic oxide yttria-stabilized zirconia (YSZ) is an established model system for spintronics research, in particular, for the heteroepitaxial integration with the ferromagnetic oxide EuO.^{1,2} Ultrathin EuO has the unique property to filter electron currents according to their spin orientation by a highly effective spin-dependent tunneling process.^{3–6} Due to the perfect lattice match of $(a_{\text{YSZ}} - a_{\text{EuO}})/a_{\text{EuO}} = -0.43\%$ ² and high thermodynamic stability, YSZ (001) is an ideal substrate for studying the structural, chemical, and magnetic properties of ultrathin EuO tunnel barriers with outstanding single-crystalline quality.

On the experimental side, the synthesis of high quality single-crystalline EuO films on YSZ (001) is conducted by reactive molecular beam epitaxy (MBE) techniques.^{2,7,8} A throughout characterization of the EuO/YSZ (001) model system, however, is hampered by the electrically insulating properties of pristine YSZ due to its large band gap of $E_{\text{gap}} \geq 4.9$ eV.^{9–11} Thus, a variety of characterization techniques based on a high electron fluence—such as electron diffraction or microscopy, or photoemission spectroscopy—are not applicable at/below room temperature due to charging effects. An advanced characterization of the EuO/YSZ (001) model system or other YSZ (001)-based oxide heterostructures therefore requires to increase the macroscopic electrical conductivity of YSZ (001), while maintaining the single-crystalline surface structure in order to allow for the heteroepitaxial growth of oxide multilayers.

Regarding its thermoelectrical properties, YSZ is a combined electronic and ionic conductor at elevated temperatures above 500 °C.¹² At room temperature, however, a high density of donors states—e.g., from metallic dopants—must be induced in order to form electronic donor states around E_F and enable electron hopping transport.¹³ Two

mechanisms may be considered for the generation of a macroscopic conductivity in YSZ at room temperature:¹⁴ (i) The creation of oxygen vacancies $V_{\text{O}}^{\bullet\bullet}$ from neutral oxide sites $\frac{1}{2}(\text{ZrO}_2) \xrightarrow{\text{ox. vac}} \frac{1}{2}\text{O}_2 + n \cdot V_{\text{O}}^{\bullet\bullet} + n \cdot 2e^-$ and (ii) the substitution of Zr by Y ions in order to generate free electrons, $\text{Zr}^{4+} \xrightarrow{\text{subst.}} \text{Y}^{3+} + e^-$.

In this study, we present at thermochemical treatment that significantly increases the macroscopic electrical conductivity of otherwise insulating YSZ (001) by the creation of oxygen vacancies $n \cdot V_{\text{O}}^{\bullet\bullet}$ and demonstrate a sizeable metallic reduction of Zr cations. The surface crystalline structure of the resulting “conductive” YSZ (cYSZ) thereby remains basically unaffected, whereas the chemical reduction of Zr oxidation states was identified by soft- and hard X-ray photoemission spectroscopy ((HAX-)PES). Moreover, ultrathin EuO magnetic oxide films were epitaxially integrated with cYSZ (001) and prove the single-crystalline quality by reflection high-energy electron diffraction (RHEED) intensity oscillations and low-energy electron diffraction (LEED). The employed characterization techniques are based on a high electron fluence and thus require a sizable sample conductivity, as is provided by thermochemically treated cYSZ (001).

In order to generate “conductive” cYSZ (001) substrates—with a significantly smaller resistivity ρ compared to pristine YSZ (001) substrates—we developed an *in situ* process consisting of successive annealing and electron bombardment steps. We start from commercial single-crystalline 10%-yttria-substituted ZrO_2 crystals (YSZ), which are cleaned by isopropanol, introduced into UHV and annealed at $T_S = 600$ °C. Next, those YSZ (001) substrates are bombarded by high-kinetic energy electrons emitted from a tungsten filament,¹⁵ which are accelerated by a voltage of $U = 1000$ V from 5 mm distance onto the YSZ substrate’s back side, as schematically depicted in Fig. 1(a). The

^{a)}Electronic mail: mart.mueller@fz-juelich.de

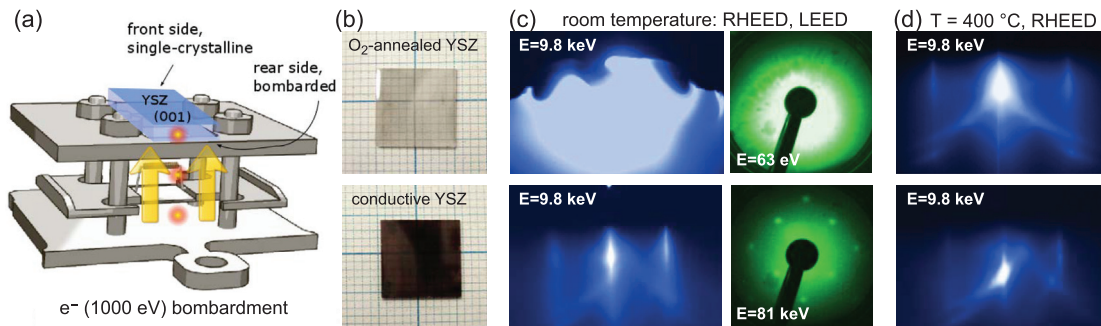


FIG. 1. (a) *In situ* e-beam treatment from the back side generates “conductive” cYSZ while protecting the polished surface. (b) Pristine and cYSZ samples. (c) and (d) Characterization by LEED and RHEED. LEED (green) is only observable on cYSZ.

electron emission current is regulated to not exceed ~ 20 mA. This hot electron bombardment is persistently applied for 2 h at an elevated substrate temperature of $T_S = 400$ °C. In a successive annealing step, the YSZ templates are kept at $T_S = 700$ °C under UHV without electron bombardment for 3 h. Structural investigations of the cYSZ (001) front side have been performed using *in situ* RHEED, LEED and *ex situ* X-ray reflection (XRR) techniques.

We performed a depth-dependent chemical analysis using (HAX)PES by either Al $K\alpha$ X-rays ($h\nu = 1.5$ keV) or hard X-ray synchrotron radiation ($h\nu = 4$ keV) at PETRA III (P09).¹⁷ Whereas the information depth of XPS is limited to the surface region of only few Å, the use of hard X-rays provides a bulk-like information depth of up to 20 nm.¹⁶ Photoelectrons were either collected in normal emission geometry $\alpha = 0^\circ$ with a maximum escape depth $\lambda^* \propto \lambda \cos \alpha$, or under an off-normal emission angle $\alpha = 45^\circ$ in order to enhance the surface-sensitivity. For a quantitative evaluation of the PES spectra, we subtracted Tougaard backgrounds and fitted by convoluted Gaussian–Lorentzian peak shapes.

In order to investigate e-beam treated cYSZ (001) as substrates for oxide heteroepitaxy, ultrathin films of the magnetic oxide EuO were grown by reactive MBE under UHV conditions. Stoichiometric EuO was synthesized by applying the Eu distillation condition at elevated substrate temperature.^{2,7,18} First, we start the Eu metal deposition, immediately followed by a meticulous regulation of an oxygen supply in the 10^{-9} millibar regime. The samples are (finally) capped with 4 nm Si for air-protection.

In Fig. 1(b), we compare a YSZ (001) substrate before and after the *in situ* conductivity treatment and observe its color changing from transparent (YSZ) to black (cYSZ). This effect is a clear indication for a modification of the material’s macroscopic electrical conductivity, with metallic donor states located in the optical band gap acting as multiple absorption channels for visible light. We probed the macroscopic electrical resistivity ρ of the substrates by two-terminal measurements and extracted averages of $\rho_{\text{YSZ}} \geq 350$ M Ω m vs. $\rho_{\text{cYSZ}} = 32.7 \pm 3$ M Ω m. Thus, we reduced the electrical resistivity of YSZ by $\sim 90\%$ by the *in situ* electron bombardment under high voltage.

Next, we investigate the surface crystalline structure of the cYSZ (001) sample front side, which is a crucial parameter for its use as substrate for oxide heteroepitaxy. In Fig. 1(c), LEED and RHEED experiments on pristine YSZ (001) show

large charging effects, which make a structural analysis impossible. Only by increasing the substrate temperature to $T_S = 400$ °C, the *fcc* (001) lattice planes become qualitatively observable by RHEED. For the conductivity-treated cYSZ (001) substrates, in contrast, the surface crystalline structure can be easily monitored by both LEED and RHEED (Figs. 1(c) and 1(d)), even at room temperature. The experimental cYSZ (001) lattice parameter is determined as $a_{\text{cYSZ}} = 5.14$ Å in an *fcc* structure, unchanged from the YSZ reference value. We can therefore conclude, that the surface crystalline quality of the cYSZ (001) front-side remains basically unaffected by our e-beam conductivity treatment.

In a further step, we aim at correlating the change of the YSZ macroscopic electrical conductivity with the microscopic electronic properties. Any induced metallicity will be directly reflected by a valence change in the cationic constituents of YSZ. Indeed, photoemission experiments (XPS and HAXPES) of pristine and “conductive” YSZ samples reveal a significant change in the oxidation state of Zr cations

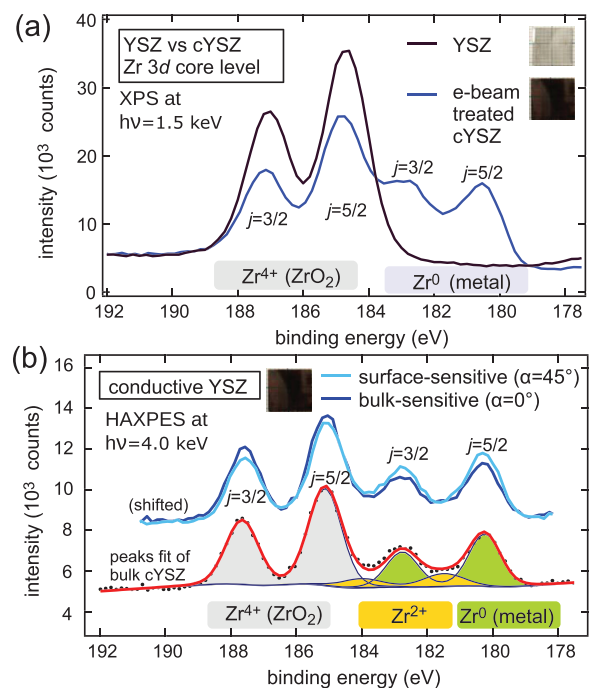


FIG. 2. Electronic structure analysis of the Zr 3d doublet in cYSZ by (a) soft X-ray PES and (b) HAXPES. In (b), depth-sensitive scans reveal a sizeable and homogeneous distribution of reduced, metallic Zr^0 spectral weight.

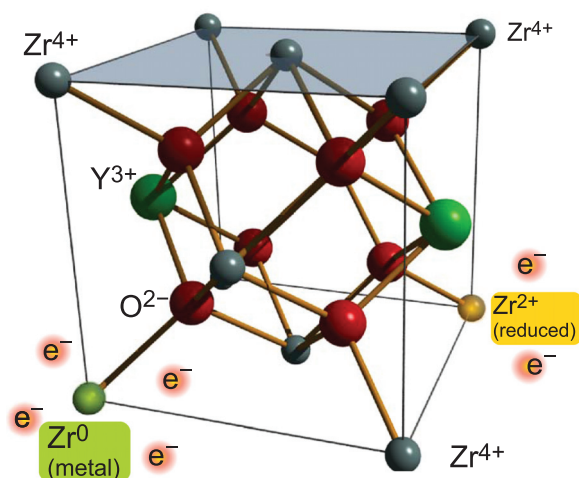


FIG. 3. Schematic illustration of the chemical reduction of Zr cations leading to a macroscopic electronic conductivity in e-beam-treated YSZ (001) substrates.

(Fig. 2). We compare the Zr 3*d* photoemission doublet of YSZ before and after the electron treatment: While in the pristine YSZ, we identify only the fully oxidized Zr⁴⁺ valence state as expected for ZrO₂ (Fig. 2(a)), in cYSZ a metallic fraction of 31.2% Zr⁰ fully and 9.8% Zr²⁺ partially reduced Zr cations are determined by a peak fitting analysis (Fig. 2(b)). We furthermore conducted a depth-dependent HAXPES experiment with varying photoelectron emission angle ($\alpha = 0^\circ$ and 45°). The Zr 3*d* spectra in Fig. 2(b) clearly confirm a homogeneous Zr⁰/Zr⁴⁺ distribution within the cYSZ substrate for the accessible probing depth of up to ~ 20 nm. In that, the (HAX)PES results clearly demonstrate that a homogeneously distributed metallic fraction of $\sim 31\%$ metallic Zr⁰ can be created in YSZ single-crystals by our *in situ* conductivity treatment.

The mechanism leading to this large fraction of Zr⁰ states in cYSZ may be explained by the creation of oxygen vacancies according to mechanism (i) $\frac{1}{2}(\text{ZrO}_2) \xrightarrow{\text{ox.vac}} \frac{1}{2}\text{O}_2 + n \cdot \text{V}_\text{O}^{\bullet\bullet} + n \cdot 2e^-$. As schematically depicted in Fig. 3, two oxygen vacancies $\text{V}_\text{O}^{\bullet\bullet}$ per Zr⁰ site may serve as donors for four electrons, where $n = 1$ leads to a partial reduction to Zr²⁺ and $n = 2$ to a reduction to metallic Zr⁰. The back color and macroscopic conductivity of cYSZ samples thus mainly arises from Zr electronic donor states at room temperature, rather than from mobile oxygen ions as, e.g., present in heated YSZ.¹³

We finally show the high-quality oxide heteroepitaxy of the magnetic oxide EuO on cYSZ (001) templates. During the growth of an ultrathin EuO film, we observe RHEED intensity oscillations of the specular spot in Fig. 4(a), indicative for a layer-by-layer growth mechanism. By analyzing the XRR Kiessig fringes (not shown), we identify four net planes of EuO ($d_{\text{EuO}} \approx 1.1$ nm). Both XRR fringes and RHEED pattern indicate that the roughness of the ultrathin EuO layer is below 0.5 nm. Furthermore, the magnetization curve of 1 nm ultrathin single-crystalline EuO/cYSZ (Fig. 4(b)) shows the expected 2nd order transition with a reduced Curie temperature as expected for ultrathin EuO. This example of the EuO/cYSZ (001) model system clearly demonstrates that cYSZ (001) serves as a high-quality single-crystalline template for oxide heteroepitaxy.

In summary, we successfully developed an *in situ* thermochemical treatment which induces a sizable and

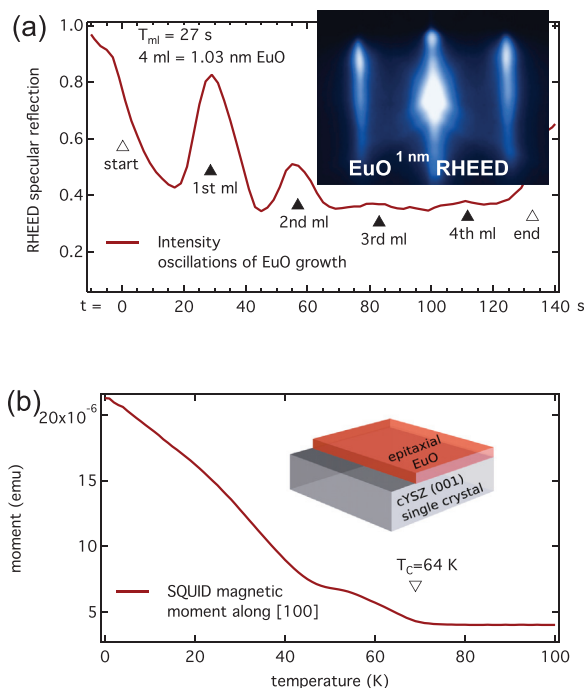


FIG. 4. (a) RHEED intensity oscillations indicate layer-by-layer EuO heteroepitaxy on cYSZ(001). The reciprocal space pattern (inset) shows the *fcc* surface structure. (b) Magnetization vs. temperature of ultrathin EuO (1 nm)/cYSZ.

homogeneous metallic conductivity in YSZ (001), as quantified by soft- and hard X-ray photoemission spectroscopy. At the same time, the surface crystalline structure remains basically unaffected, and ultrathin EuO films can be synthesized on cYSZ (100) with single crystalline quality as indicated by RHEED intensity oscillations. In that, the presented *in situ* conductivity treatment of YSZ (001) opens up a pathway for the application of various high electron-fluence characterization techniques, such as HAXPES, RHEED, and LEED, in any YSZ (001)-based functional oxide heterostructure.

The HAXPES instrument at P09 is funded by BMBF (Nos. 05KS7UM1, 05K10UMA, 05KS7WW3, and 05K10WW1). We acknowledge experimental support by T. Jansen and H. Pfeifer and funding by DFG (No. MU3160/1-1) and by HGF (No. VH-NG-811).

- ¹A. Mauger and C. Godart, *Phys. Rep.* **141**, 51–176 (1986).
- ²R. Sutarto *et al.*, *Phys. Rev. B* **79**, 205318 (2009).
- ³R. Jansen *et al.*, *Semicond. Sci. Technol.* **27**, 083001 (2012).
- ⁴M. Müller *et al.*, *Europhys. Lett.* **88**, 47006 (2009); *Appl. Phys. Lett.* **98**, 142503 (2011).
- ⁵G.-X. Miao, M. Müller *et al.*, *Phys. Rev. Lett.* **102**, 076601 (2009); *Rep. Prog. Phys.* **74**, 036501 (2011).
- ⁶C. Caspers, M. Müller *et al.*, *Phys. Rev. B* **84**, 205217 (2011); *Phys. Status Solidi RRL* **5**, 441 (2011).
- ⁷S. G. Altendorf *et al.*, *Phys. Rev. B* **84**, 155442 (2011).
- ⁸I. Moder *et al.*, *Thin Solid Films* **531**, 466–470 (2013).
- ⁹V. R. P. Verneker *et al.*, *Phys. Rev. B* **40**, 8555 (1989).
- ¹⁰O. H. Kwon *et al.*, *Solid State Ionics* **177**, 3057–3062 (2006).
- ¹¹J. H. Joo *et al.*, *Solid State Ionics* **177**, 1053–1057 (2006).
- ¹²X. Guo *et al.*, *Sens. Actuators, B* **31**, 139–145 (1996).
- ¹³B. C. H. Steele and A. Heinzl, *Nature* **414**, 345–352 (2001).
- ¹⁴K. Kobayashi *et al.*, *Solid State Ionics* **135**, 643–651 (2000).
- ¹⁵S. G. Altendorf, private communications (2012).
- ¹⁶S. Tanuma *et al.*, *Surf. Interface Anal.* **43**, 689 (2011).
- ¹⁷A. Gloskovskii *et al.*, *J. Electron Spectrosc.* **185**, 47 (2012).
- ¹⁸P. G. Steenken *et al.*, *Phys. Rev. Lett.* **88**, 047201 (2002).